



ELSEVIER

Catalysis Today 43 (1998) 233–239



Kinetics of resid hydrotreating reactions

Jie Chang^{*}, Jiansheng Liu, Dadong Li

Research Institute of Petroleum Processing (PIPP) P.O. Box 914-17, Beijing, 100083, China

Abstract

Five resids from the Middle East and China have been hydrotreated in a pilot plant, which has three fixed-bed reactors in series. Six commercial catalysts were tested. The process conditions were 12.0–16.8 MPa, 370–405°C, LHSV of 0.15–1.0 h⁻¹, H₂/oil ratio of 400–1000 nm³ m⁻³. The feedstocks included the following Chinese resids Shengli, Xinjiang and Liaohe. Kinetic parameters of resid hydrotreating reactions were calculated in terms of pore diffusion resistance and were correlated with some special properties of oils and catalysts. This study supplies important basic data for the selection of catalysts, for the design of composite catalyst beds and for the optimization of process conditions. Published by Elsevier Science B.V.

Keywords: Kinetics; Reaction; Hydrotreating; Resid

1. Introduction

Resid hydrotreating plays an important role in the modern oil refining industry. Much research has been carried out on resid hydrotreating reactions, but little has been conducted on the kinetics of Chinese resid hydrotreating reactions, especially with Xinjiang and Liaohe resids. In order to supply feedstock for RFCC (resid fluid catalytic cracking), we have done some pilot plant research on the hydrotreating kinetics of five typical resids. The relationships between hydrotreating performance and catalyst properties have been obtained. The kinetics give important information for the development of special catalysts and the design of composite catalyst beds.

2. Experimental

The hydrotreating tests of resids were conducted in a three fixed-bed reactor pilot plant. The liquid and gas

were fed downflow through the three reactors continuously. A liquid sample could be withdrawn from the outlet of each reactor. After preheating, the mixture of oil and hydrogen were fed to the reactors where hydrotreating was carried out. The hydrotreated oil was separated from the gas phase in a high pressure separator, flowed into a stabilizer, and then to a product vessel. The separated gas was scrubbed, and then was reused as recycle hydrogen. All product samples were taken after running 200 h. The reaction conditions were 370–405°C, 12.0–16.8 MPa, LHSV of 0.15–1.0 h⁻¹, H₂/oil ratio of 400–1000 nm³ m⁻³.

Five resids were used. Feed A is an Iranian AR (atmospheric resid). It has a high V (vanadium) content, low N (nitrogen) content and high S (sulfur) content. Feed B is a Liaohe AR, which has a high Ni (nickel) and N content but low S content. Feed C is a mixture of Xinjiang VR (vacuum resid) (50 wt%) and Qinghai VR (50 wt%), which has high V content, low S and N content. Feed D is a mixture of Shengli VR (80 wt%) and CGO (coker gas oil) (20 wt%), which has high Ni, N and S contents. Feed E is a

^{*}Corresponding author.

Table 1
Properties of feedstocks

Feed	Iranian ^a AR	Liaohu AR	Xinjiang/Qinghai 50/50 VR	Shengli VR 80%+CGO 20%	Arabian ^b /Iranian 60/40 VR
Label	A	B	C	D	E
API ^o	14.7	12.3	16.1	13.9	10.4
Viscosity (100°C), mm ² s ⁻¹	47.6	425.3	231.3	388.7	506.0
CCR, m%	9.6	13.4	13.7	13.0	17.5
Ultimate analysis					
S, wt%	2.90	0.40	1.28	1.45	3.3
N, wt%	0.50	0.62	0.47	1.01	0.53
C, wt%	85.37	87.28	86.34	85.42	84.90
H, wt%	11.27	11.70	11.55	11.17	10.51
Ni, ppm	30.4	93.7	21.3	46.1	36.9
V, ppm	107.0	2.4	59.7	3.1	100.0
Compositions					
Saturates, wt%	30.7	30.3	28.2	18.0	15.9
Aromatics, wt%	42.5	25.8	35.5	31.6	49.4
Resins, wt%	23.7	40.9	31.9	48.0	29.2
Asphaltenes (C ₇), wt%	3.1	3.0	4.4	2.4	5.5
Viscosity parameter					
<i>b</i>	9.8482	10.3552	10.0238	10.3898	10.1618
<i>n</i>	-3.741	-3.863	-3.752	-3.879	-3.783

^a From Iranian heavy crude.

^b From Arabian light crude.

mixture of Arabian VR (60 wt%) and Iranian VR (40 wt%).

The properties and compositions of the feedstocks are presented in Table 1. The resids were analyzed by separation into four groups on the basis of solubility and polarity. Asphaltenes were insoluble in *n*-heptane. The corresponding soluble part was separated by an Al₂O₃ Chromatography column into three components: saturates, aromatics and resins. It can be seen from Table 1 that Xinjiang resid is obviously different from other Chinese oils, because the V content is higher than the Ni content, like Middle East crudes. Liaohu AR has a high density, viscosity, metal content and resins content. It has similar characteristics of VR in many aspects. The aromatics content of Chinese-based resids is lower than that of Middle East-based resids, but the resins content of the former is higher. The CCR (Conradson carbon resid) content of Feed A is less than that of the other four. In order to hydrotreat these resids into suitable RFCC feedstocks, appropriate catalysts and processing conditions were selected guided by the hydrotreating kinetics of the various resids.

Table 2 shows some properties of the commercial catalysts used in this research. Catalysts A–C are three kinds of HDM (hydrodemetallization) catalysts. Catalysts D–F are HDS (hydrodesulfurization) catalysts. Compared with HDS catalysts, HDM catalysts have bigger pore volumes and smaller surface areas. The average pore diameters in HDM catalysts are between 10 and 20 nm, but they are less than 10 nm in HDS catalysts.

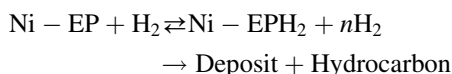
3. Background of data processing

The removal of V, Ni and S is the main target of hydrotreating. The metalloporphyrin compounds account for 30–50 wt% of metals in oils. Kinetic studies with individual metalloporphyrin model compounds indicate that the mechanism of HDM involves some intermediates. Agrawal [1] proposed that a reversible hydrogenation step of a Ni–EP to form a Ni–EPH₂ was followed by an irreversible hydrogenolysis resulting in the fragmentation of the porphyrin ring and deposition of the metal on the catalyst. The

Table 2
The properties of catalysts

Function Catalyst	HDM			HDS		
	A	B	C	D	E	F
Surface area, m ² g ⁻¹	140	164	141	151	188	268
Pore volume, cm ³ g ⁻¹	0.64	0.66	0.70	0.40	0.53	0.59
Packed density, g cm ⁻³	0.545	0.536	0.616	0.850	0.676	0.668
Pore diameter distribution, %						
<10 nm	12.1	14.7	2.3	65.7	61.2	78.0
10–20 nm	74.2	69.9	82.6	32.7	34.1	21.0
20–40 nm	11.9	13.2	14.8	1.2	3.9	0.8
40–60 nm	1.8	2.2	0.3	0.4	0.8	0.2
Average pore diameter, nm	14.6	11.7	17.0	8.3	8.5	6.5
Shape	Cylindrical	Trilobe	Trilobe	Cylindrical	Trilobe	Trilobe

reaction network was:



The same mechanism was also proposed for VO–EP. Although the kinetic parameters of individual metalloporphyrin hydrogenation can be calculated with the above mechanism, the HDM of resid cannot be treated in the same way, because not only metalloporphyrin, but also non-porphyrin metal compounds exist in resids. With this model, many parameters need to be calculated and it may not express the real reactions in resid hydrotreating. Experimentally, however, the overall HDM rate was pseudo-first-order. HDM reactions of resids have been modelled with first-order kinetics in much of the literature.

We developed a pseudo-first-order reaction model for HDM of resids. Average molecular weight was used in this model to estimate some properties of the resid. Due to large molecules of resid, their intrinsic reactivities in hydrotreating conditions are relatively high; diffusional limitations to the inherent kinetics of HDM readily occur [2]. The assumptions of this model are listed as the following:

1. The fixed-bed reactors are plugflow in gas and liquid.
2. The reactions are isothermic at the catalyst pellet level [3].
3. There is no pressure difference between the inlet and outlet of the reactor.
4. The film mass transfer resistance is negligible.

5. H₂/resid remains at the solubility equilibrium.

According to the above assumptions, the differential equation of material balance in the reactor bed is given [4] by:

$$\frac{d^2C}{dy^2} - \frac{k}{D_e} C = 0 \quad (1)$$

The boundary conditions are:

$$C = C_0 \text{ at } y = 0; \quad dC/dy = 0 \text{ at } y = L$$

Solving Eq. (1), the reaction rate of HDM is expressed as:

$$-r = kC_0\eta \quad (2)$$

where,

$$\eta = \tan h(mL)/(mL)$$

$$mL = L\sqrt{\frac{k}{D_e}}$$

For strong pore diffusion,

$$-r = \sqrt{\frac{kD_e}{L}} C_0 \quad (3)$$

The material balance in the whole reactor is expressed as:

$$V_L C_0 dx = (-r)(1 - \varepsilon_b) dV \quad (4)$$

In Eq. (4), x means fractional conversion. For example,

$$x_V = ((V \text{ in feed} - V \text{ in product})/V \text{ in feed})$$

The solution of Eq. (3) is

$$\ln\left(\frac{1}{1-x}\right) = \frac{k(1-\varepsilon_b)}{\text{LHSV}} \times \frac{\tan h(mL)}{mL} \quad (5)$$

D_e [5] is calculated by Eq. (6).

$$D_e = \frac{\varepsilon_p D}{\tau} \quad (6)$$

Stokes and Einstein [6] recommended the following formula:

$$D = \frac{1.05 \times 10^{-13} T}{\mu V_b^{1/3}} \quad (7)$$

Lin [7] proposed a method to estimate the viscosity of oil at high temperature and high pressure conditions by:

$$\log \log(\nu + j) = b + n \log T \quad (8)$$

In Eq. (8), the experience constants b , j and n were determined by measuring the viscosity at different temperatures: $j=0.6$ for Chinese oils, $j=0.8$ for Middle East oils. The values of b and n of these feeds are listed in Table 1.

$$\log\left(\frac{\mu}{\mu_0}\right) = \frac{P}{1000} (0.0239 + 0.01638 \mu_0^{0.278}) \quad (9)$$

In Eq. (9), μ can be expressed with $\nu/\mu=\nu/\rho$. Using

Eq. (2) through Eq. (9), the HDM kinetic constants were calculated.

It was also assumed that the HDS reaction of resid hydrotreating was first-order in Feed S content. In the same way, the HDS kinetic constants were calculated. This method provided an acceptable representation of experimental results.

4. Results

Feed A was hydrotreated with HDM catalysts A–C and HDS catalysts D–F, respectively. The operation conditions were 370–390°C, 14.0 MPa, LHSV of 0.20–0.40 h⁻¹. Reaction rate constants for HDM and HDS were calculated from our experimental data. HDM conversions (the removal of V, x_V , and the removal of Ni, x_{Ni}) from Feed A over catalysts A–C at various temperatures were obtained with these experiments. On the basis of these data, the reactant diffusivities, effectiveness factors and rate constants were calculated using Eq. (2) through Eq. (9). The results are listed in Table 3.

The natural logarithm of the rate constants at different temperatures is linear with the reciprocal absolute temperatures, which is an Arrhenius-type temperature dependency. Arrhenius plots for HDV

Table 3
Results of HDM reactions of Feed A over catalysts A–C

Catalyst	A			B			C		
Temperature, °C	370	380	390	370	380	390	370	380	390
D_e , 10 ⁻¹¹ m ² s ⁻¹	4.08	4.39	4.71	4.40	4.73	5.07	4.40	4.73	5.07
HDV									
x_V , %	84.5	90.9	96.6	91.2	95.7	98.7	88.4	92.2	93.4
η_V	0.92	0.91	0.88	0.81	0.77	0.72	0.84	0.82	0.79
k_V , h ⁻¹	0.953	1.253	1.085	1.256	1.749	2.549	1.061	1.325	1.672
k_0 , 10 ⁸ h ⁻¹		8.75			110.5			0.026	
E, kJ mol ⁻¹		110.3			122.4			78.8	
Correlation coefficient		0.995			0.993			0.991	
HDNi									
x_{Ni} , %	70.3	79.1	89.1	82.9	89.7	94.7	81.2	86.5	88.8
η_{Ni}	0.95	0.94	0.92	0.86	0.83	0.81	0.87	0.86	0.83
k_{Ni} , h ⁻¹	0.603	0.789	1.128	0.744	0.979	1.245	0.789	0.970	1.071
k_0 , 10 ⁸ h ⁻¹		14.2			3.25			0.01	
E, kJ mol ⁻¹		115.9			102.9			87.8	
Correlation coefficient		0.993			1.00			0.988	

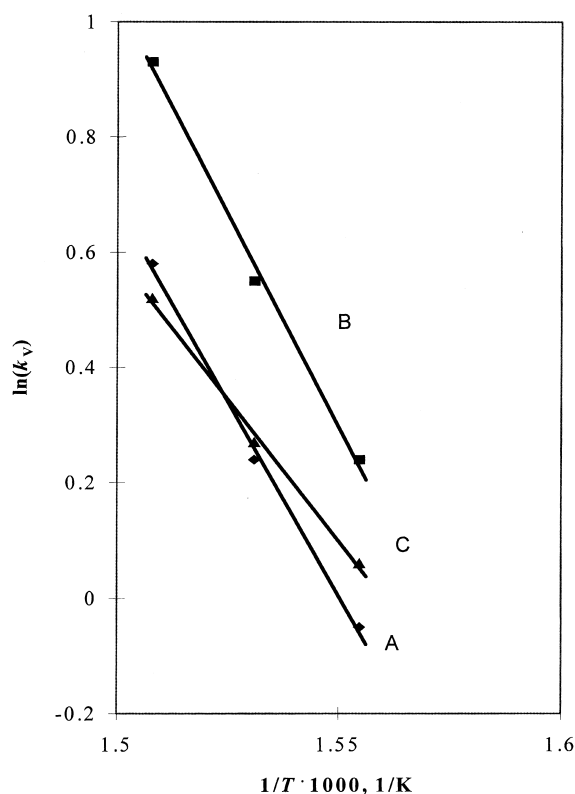


Fig. 1. Relationship between $\ln(k_v)$ and $1/T$. (A) plot for catalyst A; (B) plot for catalyst B; (C) plot for catalyst C.

and HDNi of Feed A are depicted in Figs. 1 and 2, respectively. According to the Arrhenius equation,

$$k = k_0 e^{-E/(RT)}$$

we can get its logarithm expression,

$$\ln(k) = \ln(k_0) - E/(RT)$$

E and k_0 of HDV and HDNi of catalysts A–C were calculated through linear fitting with rate constants. The value of k_0 , E and the correlation coefficient are shown in Table 3. In the same way, k_0 and E of HDS of catalysts D–F were calculated and are shown in Table 4.

From the fitted kinetic parameters and Eq. (5), the conversions of HDM and HDS at any temperature and LHSV can now be predicted. Such results are in satisfactory agreement with our experimental data; for example, the relative error of the prediction result at every condition is less than 5%.

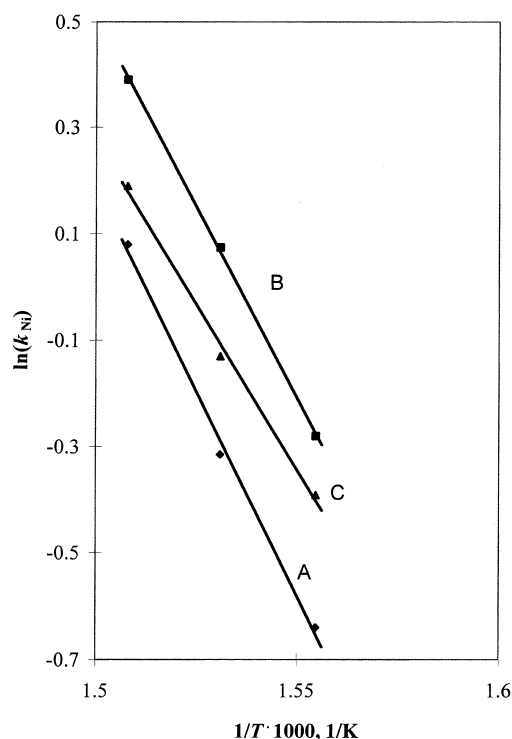


Fig. 2. Relationship between $\ln(k_{Ni})$ and $1/T$. (A) plot for catalyst A; (B) plot for catalyst B; (C) plot for catalyst C.

Feed B was hydrotreated with catalyst B at 16.8 MPa, 390–405°C. The rate constant of HDNi, labeled as BBNi (the first letter 'B' refers to Feed B, the second refers to catalyst B, 'Ni' means HDNi reaction), is listed in Table 4. The Ni component in Feed B is more difficult to remove than that in Feed A.

Feed C was hydrotreated with catalysts B and C at 16.0 MPa and 385–400°C. Rate constants for HDV, labeled as CBV and CCV, respectively, are given in Table 4. The HDV activity of catalyst B is better than catalyst C, and the rate constants are lower for Feed C than for Feed A. The rate constants at the same temperature (390°C) are shown in Table 4.

Feed D was hydrotreated with catalysts B and E at 14.7 MPa and 390–405°C. The rate constant for HDNi of catalyst B labeled as DBNi and the rate constant for HDS of catalyst E labeled as DES are also presented in Table 4. The HDNi activity is lower than that for Feed A.

Feed E was hydrotreated with catalysts A–C, respectively at 16.0 MPa. The rate constants for

Table 4

The parameters of reaction rate constants

Label	Feed	Catalyst	Reaction	$k_0, 10^8 \text{ h}^{-1}$	$E, \text{ kJ mol}^{-1}$	$k (390^\circ\text{C})^a, \text{ h}^{-1}$
ADS ^b	A	D	HDS	0.339	94.4	1.24
AES	A	E	HDS	0.0238	76.6	2.20
AFS	A	F	HDS	0.338	90.4	2.56
BBNi	B	B	HDNi	2.20	108.1	0.67
CBV	C	B	HDV	20.1	120.5	0.65
CCV	C	C	HDV	130	133.8	0.38
DBNi	D	B	HDNi	27.8	122.3	0.65
DES	D	E	HDS	0.688	100.3	0.87
EANi	E	A	HDNi	220	134.1	0.60
EAV	E	A	HDV	3914	146.1	1.22
EBNi	E	B	HDNi	840	141.7	0.58
EBV	E	B	HDV	504	136.4	0.91
ECNi	E	C	HDNi	220	132.9	0.75
ECV	E	C	HDV	52.5	123.7	0.95

^a Feed A was hydrotreated at 14.0 Mpa; Feed B was hydrotreated at 16.8 Mpa; Feed C was hydrotreated in 16.0 Mpa; Feed D was hydrotreated at 14.7 Mpa; Feed E was hydrotreated at 16.0 Mpa.

^b ADS refers to 'HDS reaction for Feed A with catalyst D'.

HDV of A–C are labeled as EAV, EBV and ECV, respectively and shown in Table 4. At the same hydrotreating conditions, temperature of 390°C, LHSV of 0.15 h⁻¹, the conversions of HDV over catalysts A–C are 99.6%, 96.0% and 97.3%, respectively.

5. Discussion

From Figs. 1 and 2, we can find that of the HDM catalysts A–C, catalyst B has the largest surface area and smallest pore diameter and is best for HDM reactions with Feed A. Catalyst A is similar to catalyst C in surface area and pore size distribution. Under the same process conditions, the catalyst with more and smaller pores is most effective for HDM reactions with Feed A, the Iranian AR. But when these catalysts are employed to hydrotreat vacuum resid at the same reaction conditions, the conversion of V in Feed E, a Middle East VR is the lowest on catalyst B. Although the V and Ni content of Feed A is similar to that of Feed E, the density, viscosity, CCR and average molecular weight of Feed E are all higher than that of Feed A. When VR is hydrotreated, catalysts with bigger pore diameters are needed. V is more easily removed than Ni in all of the feeds in this study, regardless of origin, Chinese or Middle East. Catalyst B has the highest HDM activity in treating Iranian AR,

but it shows lower HDM activity when this catalyst is used in treating Middle East VR.

Liaohu AR is similar to VR in density, viscosity and CCR. The HDM effectiveness with Liaohu AR is similar to that with Xinjiang resid, but lower than that with Iranian AR.

The V content in Xinjiang resid (Feed C) is higher than its Ni content. This feed differs from other Chinese resids, but resembles a Middle East resid. However, HDV reaction rate constant with Feed C is not only lower than that with Feed A, but also lower than that with Feed E. Compared with Chinese resids, the metal contaminants in Middle East resids are easily removed.

The above data indicate that Middle East resids, which have lower resins and higher aromatics, are more easily hydrotreated than Chinese resids with higher resins and lower aromatics. The composition of aromatics and resins in a feed probably affects its reactivity. More experiments are being done to prove this and quantify the relationships. To get satisfactory hydrotreating results, new catalysts aiming toward specific feeds must be developed.

Among HDS catalysts, catalyst F has the highest activity, because of its largest surface area and smallest average pore diameter. A catalyst that has a small average pore diameter and large surface area accelerates the hydrotreating reactions of Feed A. The HDS

rate constant of Feed D is only one-third that of Feed A at the temperature of 390°C, while the pressure of the former is higher than that of the latter. This indicates that the reactivity of Shengli resid (Feed D) is remarkably lower than that of Iranian resid during the hydrotreating.

6. Conclusions

A pseudo-first-order kinetic model which accounts for pore diffusional resistance in resid hydrotreating reactions has been developed. Results for resid hydrotreating can be predicted with this model.

At hydrotreating conditions, the properties of feeds have an important effect on their reactivities. Chinese resids are less reactive than Middle East resids. A catalyst suitable for one feedstock may not be optimum for a different feed. When hydrotreating high Ni resids and high V resids, different catalyst types should be selected. The preceding results are useful for the design and development of new hydrotreating catalysts and the optimization of operating conditions.

7. Nomenclatures

C	Concentration, ppm or %
D_e	Reactant effective diffusivity, $\text{m}^2 \text{s}^{-1}$
L	Equivalent length of catalyst, m
T	Temperature, K
V	Volume of catalyst, m^3

V_L	Liquid flow rate $\text{m}^3 \text{s}^{-1}$
x_{Ni}	Ni conversion
y	Distance from pore mouth
ϵ_p	Porosity
μ	Dynamic viscosity, 10^{-3}Pa s
τ	Pore shape factor
D	Reactant diffusivity, $\text{m}^2 \text{s}^{-1}$
k	Intrinsic rate constant, h^{-1}
P	Pressure, Psi
r	Reaction rate, h^{-1}
V_b	Average molecular volume, $\text{cm}^3 \text{mol}^{-1}$
x	conversion
x_V	V conversion
ϵ_b	Catalyst bed voidage
η	Effectiveness factor
ν	Kinematic viscosity, $\text{mm}^2 \text{s}^{-1}$
ρ	Density of oil, g cm^{-3}

References

- [1] R. Agrawal, J. Wei, *Ind. Eng. Chem. Process Des. Dev.* 23 (1984) 505.
- [2] K.W. Limbach, J. Wei, *AIChEJ.* 34 (1988) 305.
- [3] H. Toulhoat, R. Szymanski, J.C. Plumail, *Catal. Today* 7 (1990) 531.
- [4] O. Levenspiel, *Chemical Reaction Engineering*, 2nd edn., Wiley, New York, 1965, 470 pp.
- [5] G.T. Chen, *Chemical Reaction Engineering*, Chemical Industry Press, 1986, 182 pp.
- [6] C.N. Satterfield, *Masstransfer in Heterogeneous Catalysis*, MIT Press, Cambridge, MA, 1980, 21 pp.
- [7] S.X. Lin, *Petroleum Refining Engineering (I)*, 2nd edn., Petroleum Industry Press, 1990, 73 pp.